Active Guidance of a Handheld Micromanipulator using Visual Servoing

Brian C. Becker, *Student Member, IEEE,* Sandrine Voros, Robert A. MacLachlan, *Member, IEEE,* Gregory D. Hager, *Member, IEEE,* Cameron N. Riviere, *Member, IEEE*

***Abstract*—In microsurgery, a surgeon often deals with anatomical structures of sizes that are close to the limit of the human hand accuracy. Robotic assistants can help to push beyond the current state of practice by integrating imaging and robot-assisted tools. This paper demonstrates control of a handheld tremor reduction micromanipulator with visual servo techniques, aiding the operator by providing three behaviors: snap-to, motion-scaling, and standoff-regulation. A stereo camera setup viewing the workspace under high magnification tracks the tip of the micromanipulator and the desired target object being manipulated. Individual behaviors activate in task-specific situations when the micromanipulator tip is in the vicinity of the target. We show that the snap-to behavior can reach and maintain a position at a target with an accuracy of 17.5 ± 0.4µm Root Mean Squared Error (RMSE) distance between the tip and target. Scaling the operator's motions and preventing unwanted contact with non-target objects also provides a larger margin of safety.**

I. Introduction

MICROMANIPULATORS aid surgical operations by providing extremely precise movements on a small scale. Features such as remote control, force feedback, motion-scaling, and virtual fixtures enable advanced behaviors that an unassisted human would find difficult to replicate. Of particular interest is biology and microsurgery, where very delicate operations must be performed precisely on structures with cross sections varying from millimeters down to microns. Tools like the Steady-Hand [1] help surgeons by suppressing tremor or involuntary hand movement on the order of 50-100 micrometers (µm).

The precision of the surgical gesture and the comfort of the surgeon during the operation can also be improved by exploiting domain specific knowledge, using pre-operative data to design augmented reality systems for biomicroscopy [2, 3] and real-time tracking of surgical instruments and anatomical targets [2] to further improve the precision of the gesture. This information can then incorporate more intelligent behavior into the micromanipulator, such as commanding the tip to reach a target or avoiding anatomical targets that could lead to complications in the surgery. For example, [4] derives a controller for gene injection into a 90 µm diameter oosperm under 100X magnification using a single camera to servo the micro-injector using visual feedback. With a stereo camera setup, the system developed by [5] servos the micromanipulator to inject a sesame seed viewed under a 20X microscope.

Our lab has developed a fully handheld active micromanipulator called Micron whose capabilities include basic tremor suppression and motion scaling [6]. The central problem addressed in this paper is the control of the endpoint of a manipulator to perform tasks relative to an observed point or surface in space. We propose to introduce three behaviors that incorporate domain-specific knowledge and visual feedback to give the surgeon guidance in specific tasks: snap-to, motion-scaling, and standoff-regulation. One of the main challenges in doing so is the optical system involved is a microscope: at such high magnifications, the standard calibration techniques commonly used, such as [7], yield unsatisfactory results.

In the remainder of this paper, these three behaviors and their workings are explored. Section II overviews Micron and background material in using visual feedback for servoing. Section III describes the design of the system to achieve the desired behaviors. In Section IV, experiments are carried out to validate the accuracy and robustness of the visual servoing. Finally, section V discusses the results and conclusion.

II. Background

Micron (Fig. 1) is a handheld micromanipulator with piezoelectric actuators built into the handle of the tool. The

Fig. 1. Fully handheld active Micron micromanipulator

Manuscript received September 15, 2008. This work was supported in part by the National Institutes of Health (R21 EY016359), the American Society for Laser Medicine and Surgery, the National Science Foundation (EEC-9731748 and Graduate Research Fellowship), and the ARCS Foundation.

B. C. Becker is with the Robotics Institute, Carnegie Mellon University, Pittsburgh, PA 15213 USA (e-mail: briancbecker@cmu.edu).

S. Voros is with the Computer Science Department, Johns Hopkins University, Baltimore, Maryland (e-mail: svoros@cs.jhu.edu).

R. A. MacLachlan is with the Robotics Institute, Carnegie Mellon University, Pittsburgh, PA 15213 USA (e-mail: ram@ri.cmu.edu).

G. D. Hager is with the Computer Science Department, Johns Hopkins University, Baltimore, Maryland (e-mail: hager@cs.jhu.edu).

C. N. Riviere is with the Robotics Institute, Carnegie Mellon University, Pittsburgh, PA 15213 USA (e-mail: camr@ri.cmu.edu).

actuators can position the endpoint, or tip, within a roughly cylindrical shaped space with a 500 µm diameter. An external measurement system called ASAP (Apparatus to Sense Accuracy of Position) supplies Micron with real-time position and pose information accurate to ~4 ± 2 µm [8]. In addition to the X, Y, and Z location of the Micron tip, the 3x3 rotation matrix defining the pose of the instrument can be obtained. Another useful measurement available is the center position, or where the tip would be nominally pointing if the piezoelectric actuators were not active. ASAP uses position-sensitive detectors (PSD's) to detect four pulsed LEDs mounted inside diffuse spheres on the shaft of the instrument. This allows Micron to perform basic tremor suppression and motion-scaling functionalities. See Fig. 1 and 2 for the setup.

A. *Problem Definition*

The ASAP measurement system provides very fine positioning information of the instrument and allows for general tremor compensation via filtering in the frequency domain. However, it has no knowledge of what an operator sees in the microscope. Thus, the current Micron system cannot attempt to keep the tip aligned with a vein or to maintain a safe distance from anatomical features. The core issue addressed here is controlling the tip of Micron based on observations made with a stereo camera to effect three behaviors: snap-to, motion-scaling, and standoff-regulation.

The first behavior, snap-to, involves guiding the Micron tip to a 3D point in space and maintaining the tip at that location. Snap-to can be thought of as a more constrained version of tremor suppression and is useful when the tip must be held stable, i.e. for injections. The second behavior, motion-scaling, is more practical when very precise movements are needed. Every movement made by the operator is scaled by a user-defined fraction, thus reducing positioning errors. The finite range of the actuated tip limits when motion scaling can be applied, so it is only turned on when in the vicinity of the target. The final behavior, standoff-regulation, serves as a preventative measure against accidental, unwanted contact. In this mode, Micron can attempt to avoid bringing the tip in contact with points by repulsing it within a preset distance of the "off-limits" areas. Each behavior has unique properties that can benefit a surgeon in different circumstances.

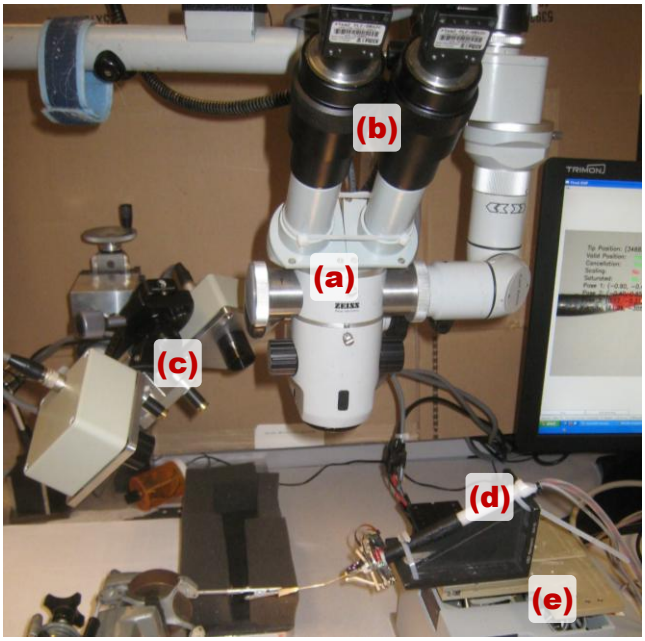

Fig. 2. System setup. (a) Microscope, middle center. (b) Cameras, top center. (c) ASAP measuring system, middle left (d) Micron, bottom right, attached to (e) Hexapod micropositioner.

B. *Visual Servoing*

Visual servoing is a popular approach to guiding a robotic appendage or manipulator using visual feedback from cameras [9]. Given a target pose or position that the robot is to reach, the goal of visual servoing is to minimize the following error:

$$e(t) = s(m(t), a) - s^* \qquad (1)$$

where s^* represents the desired positions, $s(m(t), a)$ the measured positions, $m(t)$ the measured feature points in the image, and a any external information needed (such as camera parameters). In general, $s(m(t), a)$ is usually the endpoint, or tip, of the manipulator. The tip position is determined from $m(t)$, the image coordinates of the tracked tip, and a, the camera mapping between world space and the image coordinates. In practice, s^* may not be known a-priori and instead be calculated from image features as well.

The approach used to minimize the error $e(t)$ can be done in one of two general ways: position based visual servoing or image based visual servoing [9, 10]. Image based servoing uses an *image Jacobian* or *interaction matrix* to convert errors measured in the image directly into a velocity the robot should attempt to maintain. In contrast, position based servoing treats the camera system as a 3D position sensor and measures the error in the task space rather than in the image. In the case of controlling only the translation of a tool, as is the case with the 3 Degrees Of Freedom (DOF) Micron micromanipulator, [11] proves these two approaches are equivalent. Therefore, this research chooses to use the position based visual servoing approach because of the well-defined positioning system provided by ASAP and the ability to run calibration routines online. Furthermore, implementing the standoff regulation requires distance metrics in 3D space.

C. *Novelty Considerations*

Micron has several specificities that differentiate the system from a typical visual servoing setup. First, Micron is not a fully autonomous robot in the sense that it has a limited range of motion that is determined by the user operating the micromanipulator. The operator may move

Micron to a position where the target cannot be reached by the tip of the instrument. Second, an external measurement system is available which allows for online calibration of the system, either before each run or during the run. Third, unlike a purely closed-loop system, Micron has to account for human dynamics involving the human's eye-hand coordination feedback loop. Other research, mainly [12], explicitly consider control with a human user in micromanipulation, but only for the purposes of high level task sharing and direction. For the majority of this paper, interaction with the human controller will not be explicitly considered in order to give a more complete characterization of the system's performance in the context of visual servoing.

These novel problems must be eventually resolved, and thus the results will be evaluated and discussed with these considerations in mind.

III. System Design

ASAP and Micron are integrated on a real-time LabVIEW® target machine with the ASAP measuring system running in parallel with the controller. The Micron interface and vision system run on a standard Windows® PC that is networked to the real-time machine to retrieve ASAP positioning information, perform stereo visual servoing, and send control signals back to Micron.

A. Visual Feedback

Designed for microsurgical work, Micron is operated under a high-power Zeiss® OPMI® 1 microscope with a magnification often exceeding 25X and a visual workspace often only several millimeters in diameter. Two PointGrey Flea2 cameras capturing 800x600 video at 30Hz are mounted to the microscope, providing a stereo view of the workspace. Each camera view is approximately 2x3 mm with each pixel corresponding to ~3.4 µm.

The micromanipulator tip and feature landmarks are tracked in both views, giving a stereo reconstruction of the instrument tip relative to the targets. Since advanced tracking is not the topic of this research, the tip and target are marked with different colored paint for easy visual identification. Tracking is performed with a simple, but robust color tracker [13]; the highly optimized and popular Intel® OpenCV library is used for implementing the computer vision techniques.

B. Micromanipulator Control

The chief control problem is how to use visual servoing in the context of Micron; in other words, given the tracked tip and target position, how can a control signal be derived in world, or ASAP, coordinates? The fundamental perspective camera equation is $p = MP$ where P is a 4x1 homogenous point in 3D world coordinates that is projected to p, a homogenous 3x1 image coordinate by the 3x4 camera matrix M. M is derived in the following section and defines the projective mapping between ASAP and the cameras. A second camera observes the same point P, creating a joint observation system defined by the fundamental perspective camera equation for each camera: $p_1 = M_1 P$ and $p_2 = M_2 P$. These equations can be combined and solved using the homogenous linear triangulation method described in [14]. Thus, as seen in Fig. 3, each set of the 2D points in the stereo pair will yield an acceptable back-projected 3D point.

Now that the tracked tip and target image locations have been reconstructed as 3D points in the ASAP workspace, the goal is to drive the error $E = P_{tip} - P_{target}$ to zero by controlling the endpoint velocity of the tip. When the error is zero, the tip and target should be coincident. The velocity can be determined as a proportion λ of the error:

$$v = \lambda(P_{tip} - P_{target}) \qquad (2)$$

Because velocities command the motion of the tip, errors due to errors in the calibration are absorbed with each new velocity calculation and drive E asymptotically to zero even in the presence of calibration errors.

C. Calibration

Currently, control of Micron operates in the coordinate system defined by the ASAP measurement system. However, the control signals are derived from the tracked tip and target viewed in the stereo camera setup. Furthermore, any preoperative information is usually registered in the image reference system. Thus calibration mappings M_1 and M_2 for camera one and two respectively are needed to transform from pairs of 2D image coordinates p_1 and p_2 to a 3D world coordinate point P.

In visual servoing, only the rotation mapping is important as translation is handled by streaming many sequential velocities to guide the tip in the direction of the target. However, because ASAP provides very accurate positions of the tip in 3D world coordinates, the full perspective mapping can be obtained. Furthermore, the full perspective camera mappings are useful because they can provide the visual trackers a rough estimation of where the

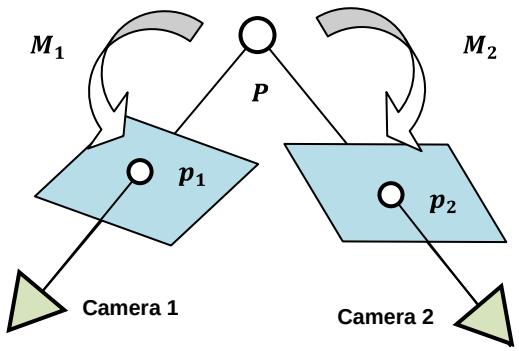

Fig. 3. Multiple view camera geometry, showing the projective relationship M_1 and M_2 that map the 3D point P to image coordinates p_1 and p_2 viewed by two cameras. Note this is for the general case; the cameras views in the Micron setup are parallel.

tip is in the image. This reduces the amount of processing time required to locate the tip in the image, yielding increased framerates and better control performance.

A corresponding set of 3D world coordinates P_i and 2D image coordinates p_{1i} and p_{2i} form an over-determined system of equations $p_{1i} = M_1 P_i$ and $p_{2i} = M_2 P_i$, which can be solved by $M_1 = p_{1i} P_i^+$ and $M_2 = p_{2i} P_i^+$ where P_i^+ denotes pseudo-inversion. A method that is more robust is the Direct Linear Transformation algorithm from [14]. This yields the pinhole camera perspective parameters, allowing a two way mapping between 2D image coordinates and 3D ASAP coordinates.

Calibration can be performed online, using the first 5-60 seconds of corresponding world and image coordinates in each run. If system positioning, magnification, and focus do not change between runs, calibrations may be reused as the visual servoing does not depend on accurate absolute calibration [15], which is cumbersome to obtain with a microscope [16]. The calibration routine involves the operator moving the tip randomly through the workspace, including up and down. A typical 60 s calibration yields approximately 2000 data points, from which outliers are automatically removed via a simple distance metric before the calculations are performed. After calibration, the 3D tip position as measured by ASAP can be projected in the image accurately within 10 pixels and the tracked tip in the stereo images can be reconstructed in 3D space with an error of about 45 ± 35 µm. Over time, the absolute calibration accumulates errors relative to ASAP as the tool pose is changed and the system shifts; however, this is not a problem as the control depends on the relative difference between the tip and target positions.

IV. Experimental Results

Three different experiments were carried out to evaluate the desired behaviors snap-to, motion-scaling, and standoff-regulation. First and foremost, the goal is to demonstrate the correctness and accuracy of each behavior. To eliminate any human-in-the-loop influences or disturbances, such as tremor, and achieve very repeatable results, all experiments requiring movement of the handheld micromanipulator were performed with the micromanipulator attached to the very precise (sub-µm) six-axis Hexapod positioning system. Since a machine will be "holding" Micron, it is equally important to evaluate the feasibility of applying these behaviors when a human is operating the micromanipulator. As such, a fourth experiment tested the helpfulness of the snap-to feature in a pointing task involving human tremor and compared it against basic tremor cancellation already implemented in Micron.

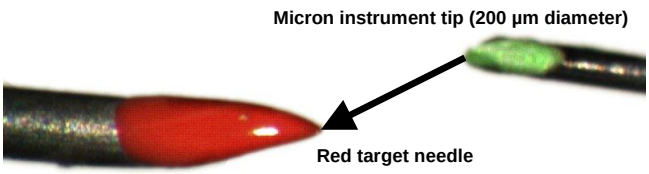

Fig. 4. Snap-to target experiment servoing Micron tip to a stationary 3D target point defined by a colored needle tip

TABLE I
Snap-To Results: Speed and Accuracy

Initial Distance (µm)	Convergence Speed (s)	Distance RMSE (µm)
375.3 ± 2.5	0.54 ± 0.02	16.6 ± 0.4
449.2 ± 5.6	0.59 ± 0.07	17.5 ± 0.4
677.9 ± 0.8	0.69 ± 0.04	18.3 ± 0.4

Speed and accuracy of servoing the tip to a 3D target from three different locations. Each location was reached three times to obtain a mean and standard deviation. RMSE measures the distance error between the tip and target for 15 s after convergence.

A. Experiment 1: Snap-To

Experiment 1 tested the snap-to functionality for convergence speed and accuracy to a stationary point. Human hand motion and tremor are rapid, necessitating a fast response time. The experiment, seen in Fig. 4, servos the Micron tip to a 3D point defined by a colored needle tip. Both the micromanipulator and target point were held stationary. The target point on the needle was rigidly held by a clamp and Micron was firmly affixed to the Hexapod; only the Micron tip was actuated. Because the Hexapod was not actively moving the Micron handle, tremor reduction was not used for this experiment.

The experiment was performed from three different starting locations with three identical runs for each location. A summary of several important statistics is listed for each location in Table 1. First, the initial distance between the tip and target is listed, as this determines convergence speed. The speed is the time taken for the tip to converge on the target with successful convergence defined as being within 25 µm of the target. Once the tip has converged, the RMSE is calculated from the 3D Euclidean distance between the tip and target during the 15 seconds after the target has been reached. Fig. 5 shows the distance error between the actuated Micron tip and the target for all three runs of the first location. The noise after convergence is caused mostly by small errors in the image trackers magnified by the backprojection into 3D. All runs exhibit similar trajectories and noise patterns.

While the convergence accuracy of the snap-to behavior is high, the convergence speed of approximately half a

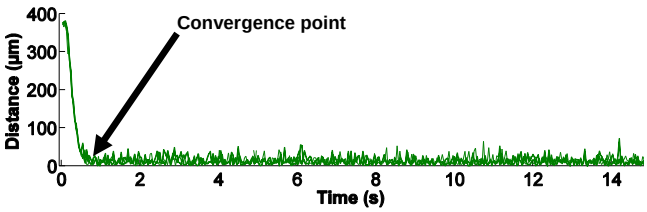

Fig. 5. Euclidean distance between Micron tip and target for three runs from the second location.

TABLE II
MOTION-SCALING RESULTS: SPEED AND ACCURACY

Initial Velocity (µm/s)	Scaled Velocity (µm/s)	Final Velocity (µm/s)	Measured Scale
95.5±1.9	62.0±0.1	96.4±0.7	1.5±0.0
91.6±4.6	43.9±4.0	91.7±8.4	2.1±0.1
95.3±1.0	30.6±0.2	96.9±0.9	3.2±0.0

Mean measured 3D velocity before coming in range of the target, while the tip is within a 170 µm radius of the target, and after the tip has passed the edge of the circle. Three runs were executed for each scale tested: 1.5, 2.0, 3.0.

second is rather slow. Once converged, the visual servoing can hold a stationary point very well, even in the presence of disturbances. For example, if the whole Micron instrument is moved, it is desirable for the tip position to actuate fast enough that it can still remain steady on the target. If the response is too slow, tremor introduced as the human user operates will result in oscillations as the tip tries and fails to keep the tip moving as fast as the tremor.

To model tremor-like movement, a disturbance signal was induced by moving the Hexapod base that Micron was attached to, in all three directions and in a roughly sinusoidal pattern. This was done without any of the tremor compensation techniques used by Micron. As shown in Fig. 6, the Micron tip remained steady even with rather large and rapid changes in position. This indicates that even in the case of rapid tremor motion, the Micron tip can remain "snapped-to" a stationary target very accurately. Experiment 4 expounds more by testing it with real tremor.

B. *Experiment 2: Motion-Scaling*

In experiment 2, the micromanipulator was moved at a constant speed in 3D space past the target point using the Hexapod micropositioner. When the tip of the instrument was detected to be within an arbitrarily chosen 170 µm radius of the target, the motion-scaling behavior was activated with a scale factor of 1.5, 2.0, and 3.0 respectively. Thus, the constant velocity of the tip should

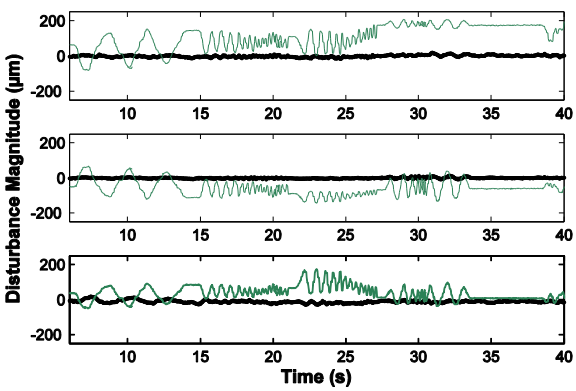

Fig. 6. Micron tip position (thick black line) snapped-to a target even with large, rapid changes in Micron instrument positioning (thin green lines) in X, Y, and Z directions (top, middle, bottom respectively).

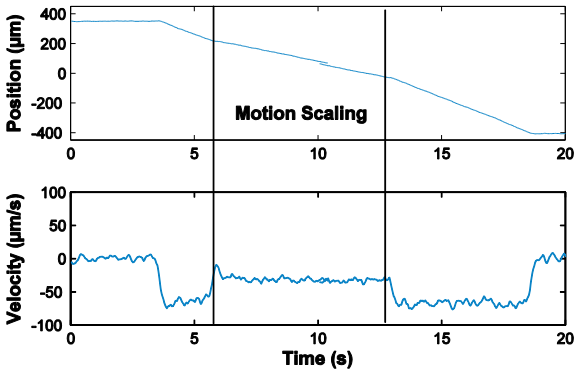

Fig. 7. Position and velocity of the Micron tip from one run as the instrument is moved with constant velocity. The middle motion scaling region represents when the tip is within range of the target.

reduce by a factor of $1/s$ while the tip is in vicinity of the target. The variability from $1/s$ will be examined to determine the effectiveness of this technique. As seen in Table II, the motion scaling works very well. There is a slight difference between the desired scale and the actual scale, but the overall variability is low. Velocity variability from time instant to time instant is influenced by the noise level and is difficult to assess accurately. Fig. 7 shows that the slopes of the position and the numerically differentiated velocity (smoothed with a 1 Hz lowpass filter) are well behaved.

C. *Experiment 3: Standoff-Regulation*

Experiment 3 validates the ability of the visual servoing controller to maintain a standoff distance from a 3D target point. In this case, instead of snapping-to, the desired action is for the tip to avoid the target. This could be useful in many surgical situations where "keep-away" points or zones might be defined to avoid unwanted and possibly damaging contact with tissue. As with the motion scaling, a spherical volume is defined around the target point in 3D. If the tip comes within a distance of 240 µm of the target, a repulsive force is exerted on the tip to guide it away. As the simplest case, the repulsive field is modeled after a charged particle; thus, the force exerted on the tip is always away

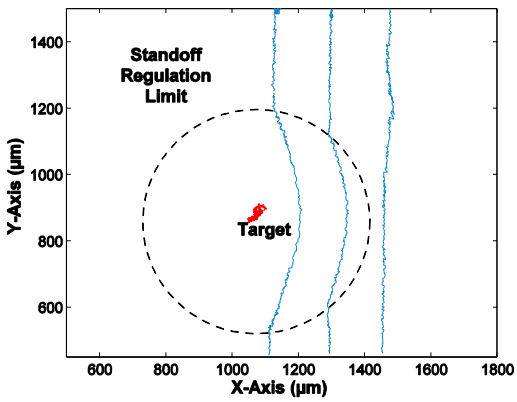

Fig. 8. Three tip trajectories, two infringing the field pushed away from their paths to maintain separation between the target and the tip.

from the center of the target. The Hexapod micropositioner is used to move the Micron tip in a straight line approaching the target at three different distances. The resulting trajectories can be viewed in Fig. 8. The standoff-regulation does push the trajectory of the tip away from the target. Additionally, the trajectory that clearly did not come near the target was unaffected. However, the simplistic model of a charged-particle is non-optimal in that it does not attempt to maintain a constant standoff.

D. Experiment 4: Pointing Task

One of the common tasks in micromanipulation is pointing, or keeping the tip steady at some target. Often, injecting a drug or chemical is the goal. Generally, tremor compensation algorithms attempt to filter out the tremor bandwidth of 8-12 Hz [17]. The research we have done in our lab suggests that there is often a lower frequency drift component in tremor. One way to rectify this drift is to know the target point about which the user is trying to keep the tip steady. Experiment 4 compares a human operator attempting a pointing task unaided, with frequency-based tremor compensation, and with the snap-to image guidance. One subject performed three runs for each scenario, attempting to keep the Micron tip steady at the 3D target position for 60s. The evaluation metric is the RMSE of distance between the target point and the Micron tip. Table III lists the results. As expected, frequency based tremor compensation performed better than unaided. The snap-to performed even better, although the error was much higher than reported earlier because Micron could not always reach the target point.

V. Discussion and Conclusion

We present a piece of a computer assisted system for microsurgery, which yields encouraging initial results in a challenging environment. Using a simple calibration routine, Micron employs visual servoing to significantly increase accuracy in pointing tasks, even over existing tremor cancellation methods. We have demonstrated finer motor control is possible locally around a target using motion scaling, and a surgeon can define "keep away" areas to help avoid unwanted tissue contact.

One issue not dealt with in this paper is the finite manipulator range. If Micron is snapping-to, the user can shift the entire manipulator out of range of the target. Because the actuators can only move a limited amount before reaching their limits, additional behavior is needed.

We plan on developing more realistic ways to track targets and surgical instruments, thereby relieving our current constraint of color tracking. Because magnification and focus can change during an operation, future work will include online routines that detect these changes and update the calibration accordingly through adaptive gains. On the control parts of the system, a more sophisticated control algorithm is needed for standoff-regulation. We also plan to perform clinical tests with human subjects to validate these behaviors aid in actual operations and surgeries.

TABLE III
Pointing-Task Results: Distance RMSE

Unaided (μm)	Tremor Compensation (μm)	Snap-To (μm)
222.9±61.3	175.8±65.9	70.1±25.9

RMSE distance between the target and Micron tip during a 60s pointing task.

References

[1] B. Mitchell, J. Koo, I. Iordachita, P. Kazanzides, A. Kapoor, J. Handa, G. Hager, and R. Taylor, "Development and application of a new steady-hand manipulator for retinal surgery," *IEEE International Conference on Robotics and Automation*, pp. 623-629, 2007.

[2] I. Fleming, S. Voros, B. Vagvolgyi, Z. Pezzementi, J. Handa, R. Taylor, and G. Hager, "Intraoperative visualization of anatomical targets in retinal surgery," in *IEEE Workshop on Applications of Computer Vision*, 2008.

[3] J. W. Berger and B. Madjarov, "Augmented Reality Fundus Biomicroscopy A working clinical prototype," *Arch Ophtalmol.*, vol. 119, pp. 1815-1818, 2001.

[4] X. Li, G. Zong, and S. Bi, "Development of global vision system for biological automatic micro-manipulation system," *IEE International Conference on Robotics and Automation*, vol. 1, pp. 127-132, 2001.

[5] H. Yamamoto and T. Sano, "Study of micromanipulation using stereoscopic microscope," *IEEE Transactions on Instrumentation and Measurement*, vol. 51, pp. 182-187, 2002.

[6] C. N. Riviere, W. T. Ang, and P. K. Khosla, "Toward active tremor canceling in handheld microsurgical instruments," *IEEE Trans. Robot. Autom.*, vol. 19, pp. 793-800, 2003.

[7] Z. Zhang, "A Flexible New Technique for Camera Calibration," *IEEE Transactions on Pattern Analysis and Machine Intelligence*, pp. 1330-1334, 2000.

[8] R. A. MacLachlan and C. N. Riviere, "High-speed microscale optical tracking using digital frequency-domain multiplexing," *IEEE Trans. Instrum. Meas.*, 2008, in press.

[9] F. Chaumette and S. Hutchinson, "Visual servo control, part I: basic approaches," *IEEE Robotics and Automation Magazine*, vol. 13, pp. 82–90, 2006.

[10] S. Hutchinson, G. D. Hager, and P. I. Corke, "A tutorial on visual servo control," *IEEE Transactions on Robotics and Automation*, vol. 12, pp. 651-670, 1996.

[11] J. P. Hespanha, Z. Dodds, G. D. Hager, and A. S. Morse, "What Tasks can be Performed with an Uncalibrated Stereo Vision System?," *International Journal of Computer Vision*, vol. 35, pp. 65-85, 1999.

[12] M. Ammi and A. Ferreira, "Involving the operator in the control strategy for intelligent tele-micromanipulation," *IEEE/ASME International Conference on Advanced Intelligent Mechatronics*, vol. 2, 2003.

[13] M. H. Yang and N. Ahuja, "Gaussian mixture model for human skin color and its application in image and video databases," *SPIE Storage and Retrieval for Image and Video Databases*, vol. 3656, pp. 458-466, 1999.

[14] R. Hartley and A. Zisserman, *Multiple View Geometry in Computer Vision*: Cambridge University Press, 2003.

[15] G. D. Hager, "A modular system for robust positioning using feedback from stereovision," *IEEE Transactions on Robotics and Automation*, vol. 13, pp. 582-595, 1997.

[16] G. Danuser, "Photogrammetric calibration of a stereo light microscope," *Journal of Microscopy*, vol. 193, pp. 62-83, 1999.

[17] R. J. Elble and W. C. Koller, *Tremor*: Baltimore: Johns Hopkins, 1990.